

Loss-Guided Auxiliary Agents for Overcoming Mode Collapse in GFlowNets

Idriss Malek ^{*,}, Abhijit Sharma and Salem Lahlou

Mohamed Bin Zayed University of Artificial Intelligence, UAE

Abstract. Although Generative Flow Networks (GFlowNets) are designed to capture multiple modes of a reward function, they often suffer from mode collapse in practice, getting trapped in early discovered modes and requiring prolonged training to find diverse solutions. Existing exploration techniques may rely on heuristic novelty signals. We propose Loss-Guided GFlowNets (LGGFN), a novel approach where an auxiliary GFlowNet’s exploration is directly driven by the main GFlowNet’s training loss. By prioritizing trajectories where the main model exhibits high loss, LGGFN focuses sampling on poorly understood regions of the state space. This targeted exploration significantly accelerates the discovery of diverse, high-reward samples. Empirically, across various benchmarks including grid environments, structured sequence generation, and Bayesian structure learning, LGGFN consistently enhances exploration efficiency and sample diversity compared to baselines. For instance, on a challenging sequence generation task, it discovered over 40 times more unique valid modes while simultaneously reducing the exploration error metric by approximately 99%.

1 Introduction

Tasks such as material design and drug discovery are fundamental to advancing essential scientific fields such as medicine [23], energy, engineering and technology [13]. However, these tasks face the challenge of exploring vast combinatorial design spaces, ranging from 10^{60} possible drug-like molecules to potentially more for functional materials, making exhaustive search infeasible. Traditionally, drug and material discovery relied heavily on time-consuming and costly experimental screening and expert-guided design. [54, 29, 12].

To overcome these limitations, machine learning has emerged as a key tool for accelerating discovery by providing proxy models [45, 9, 26] or methods to guide experiments [17, 18]. Moreover, it enabled better exploration of large combinatorial spaces efficiently by leveraging their underlying structure. Reinforcement Learning (RL) [50] is the most popular learning framework for this purpose, as it enables agents to iteratively interact with an environment to discover the single candidate that maximizes a reward, making it well-suited for tasks where the goal is to identify one optimal solution. However, in a real-world setting, a high-scoring candidate may still pose undesirable side effects or be synthetically inaccessible. Therefore, instead of identifying a single optimal solution, it is often more practical to generate a diverse set of high-quality candidates, increasing the chances that at least one will be viable in practice.

Generative Flow Networks (GFlowNets) [4] aim at learning a forward policy $P_F(a | s)$, encoding choices of actions a at partial states s , that sequentially constructs an object x with probability proportional to a given reward $R(x) > 0$. Unlike RL, which prioritizes finding the single best candidate, GFlowNets focus on generating a diverse set of high-reward samples. GFlowNets have found great success in many areas of applications, such as causal discovery [36, 14], material discovery [11, 37], drug discovery [47, 41], biological sequence design [24] and editing [16], large language model improvement [51, 21, 22], diffusion models improvement [57], scheduling [58] and combinatorial optimization problems [56]. In addition, alternative theories that extend GFlowNets to environments that are continuous [30], stochastic [40], and adversarial [25], which further expand the scope of possible applications such as an alternative to denoising diffusion models [46].

Even if GFlowNets and Reinforcement Learning have two different objectives, they share their need for exploration to achieve their goal. In sparse reward settings, an RL agent that doesn’t explore will not be able to improve its “understanding” of the environment and will converge to a suboptimal policy. In the same manner, even though they were specifically designed to capture multiple modes of a reward function, GFlowNets training strategies that lack exploration might lead the agent to get stuck in a region and make the underlying distribution incomplete. This behavior is more visible in large sparse-reward environments [35] where the agent might need to go through expansive regions with no or minimal reward.

Previous studies have aimed to enhance GFlowNet training by investigating credit assignment [34, 32, 38]. However, akin to RL, the effectiveness of GFlowNets relies on the trajectories used to explore high-reward regions. Due to this similarity, prior work on GFlowNets [39, 44, 31, 27, 33] has drawn insights from the RL literature [8, 7, 53] to develop new exploration strategies. In particular, Bengio et al. [5] briefly cite the idea of using a second GFlowNet trained mostly to match a different reward function that is high when the losses observed by the main GFlowNet are large. Building on this idea, Madan et al. [33] suggested to implement this idea by using novelty-based intrinsic rewards, whereas Kim et al. [28] directly uses the loss value of a trajectory.

In this work, we introduce a new general training strategy for GFlowNets that can be used with any training objective. Instead of using an artificial novelty-based intrinsic reward to judge how informative a trajectory is, we directly use the loss value. To avoid ruining the objective probability distribution, we use an auxiliary agent that will sample never-seen trajectories. In Sections 3 and 2, we introduce GFlowNets and review existing exploration strategies used in

* Corresponding Author. Email: malek.idriss@mbzuai.ac.ae

their training. Section 4 outlines the motivation behind our approach, details of the proposed method, and the advantages of leveraging the loss signal over traditional novelty-based intrinsic rewards. Finally, in Section 5, we show that our method matches or exceeds the previous state-of-the-art across diverse experimental settings, achieving improvements ranging from 10% in one task to 99% in another where prior methods failed entirely.

2 Background

We consider a directed acyclic graph $(\mathcal{S}, \mathcal{A})$. We refer to the nodes \mathcal{S} as states and to the edges \mathcal{A} as actions. If $(s, s') \in \mathcal{A}$, we say that s is a parent of s' and that s' is a child of s . There is a unique state s_0 that has no parents that we name source state and a unique state with no child s_f that we name sink state. We refer to the parents of the sink state as terminating states $\mathcal{X} = \{s \in \mathcal{S} \mid (s, s_f) \in \mathcal{A}\}$. A complete trajectory $\tau = (s_0, s_1, \dots, s_n, s_{n+1} = s_f)$ is a sequence of states that start with the source state and ends with the sink state.

We also consider a reward function $R : \mathcal{X} \rightarrow \mathbb{R}$ such as $\forall x \in \mathcal{X}, R(x) > 0$. By abuse of notation, we can also consider that the reward for non terminating states is zero $\forall s \in \mathcal{S} \setminus \mathcal{X}, R(s) = 0$. The goal of the GFlowNet is to learn to sample terminating states proportionally to the reward function $P_T(x) \propto R(x)$. To do this, GFlowNets start from the initial state (for example, empty molecule in drug discovery setting, initial coordinates in hyper-grid environment) and iteratively sample actions to move to the following states.

Formally, we consider a non-negative flow function $F : \mathcal{A} \rightarrow \mathbb{R}$. The goal of the GFlowNet framework is to learn such a flow function that satisfies the following flow matching (FM) and reward matching constraints:

$$\forall s' \in \mathcal{S} \setminus \{s_0, s_f\}, \quad \sum_{(s, s') \in \mathcal{A}} F(s \rightarrow s') = \sum_{(s', s'') \in \mathcal{A}} F(s' \rightarrow s'') \quad (1)$$

$$\forall s' \in \mathcal{X}, \quad F(s' \rightarrow s_f) = R(s') \quad (2)$$

We extend the definition of the flow function to states:

$$\forall s \in \mathcal{S}, \quad F(s) = \sum_{(s, s') \in \mathcal{A}} F(s \rightarrow s') \quad (3)$$

We also define the forward and backward policies as follow:

$$P_F(s' \mid s) = \frac{F(s \rightarrow s')}{F(s)} \quad (4)$$

$$P_B(s \mid s') = \frac{F(s \rightarrow s')}{F(s')} \quad (5)$$

The FM constraint ensures that for every non-terminal state s , the total incoming flow equals the total outgoing flow. Inspired by the FM objective, detailed balance (DB) condition is a stricter version that enforces equality of flows between individual state pairs as shown in Equation 6 below:

$$\forall (s, s') \in \mathcal{A} \text{ and } s' \neq s_f, \quad F(s)P_F(s' \mid s) = F(s')P_B(s \mid s') \quad (6)$$

$$\forall s \in \mathcal{X}, \quad F(s)P_F(s_f \mid s) = R(s) \quad (7)$$

In practice, DB implies FM since satisfying pairwise flow equality naturally results in balanced total inflows and outflows at each state. Therefore, the FM and DB constraints are mathematically equivalent when applied over every edge in both directions and all states [6].

Although initial work on GFlowNets focused primarily on FM and DB objectives, in this paper, we will use the trajectory balance (TB) objective to train GFlowNets. Introduced in Malkin et al. [34], the trajectory-decomposable loss only parametrizes the forward and backward policy, and add a learnable scalar Z_θ that represents the total reward:

$$\mathcal{L}_{TB}(\tau, \theta) = \left(\log \left(\frac{Z_\theta \prod_{t=1}^{n+1} P_F^\theta(s_t \mid s_{t-1})}{R(s_n) \prod_{t=1}^n P_B^\theta(s_{t-1} \mid s_t)} \right) \right)^2 \quad (8)$$

Unlike the FM objective, TB requires only trajectory-level rewards rather than fine-grained supervision at each state or transition, making it more scalable to complex environments. Similarly, compared to the DB objective, TB avoids the need to compute flows for all intermediate states explicitly and is easier to optimize in practice due to its trajectory-wise formulation. Additionally, TB naturally accommodates stochastic policies and enables learning from sampled trajectories without requiring full state space enumeration.

3 Related Work

Exploration in Reinforcement Learning: Exploration is a critical aspect of reinforcement learning (RL). Traditional methods, such as ϵ -greedy [50], optimism-based upper confidence bounds (UCB) [1], and Thompson sampling [52], often struggle in complex environments. Approaches based on counts and pseudo-counts [3] reduce the focus on frequently visited states, but they fail to scale in high-dimensional settings. Other intrinsic motivation (IM) methods leverage indirect novelty signals as intrinsic rewards. For instance, Random Network Distillation [7] uses the discrepancy between a target and a trainable neural network to capture novelty, instead of absolute novelty, NovelD [59] uses novelty difference to give large intrinsic reward at the boundary between explored and unexplored regions. Go-Explore [15] takes a different approach by storing promising states to facilitate easy returns to these regions. Other approaches also used an auxiliary agent to help the main learner improve [2, 20, 49].

Training GFlowNets: GFlowNets were introduced by [4], employing the flow-matching objective to reformulate the flow-matching and reward-matching constraints as a loss function. To improve credit assignment and stabilize training, various alternative objectives have been proposed. The detailed-balance objective [5] operates at the level of individual transitions, while the trajectory-balance objective [34] evaluates entire trajectories. Additionally, the SubTB(λ)-objective [32] enables learning from incomplete trajectories, boosting training efficiency. Recent work suggest that weighting the DB objective based on the number of terminal descendants improves the training process [48].

Exploration in GFlowNets: The success of GFlowNet training largely depends on the quality of the sampled trajectories. If training is focused on trajectories that consistently converge to a restricted region, sampling diversity can suffer. To address this, [39] introduced intrinsic rewards based on novelty methods [7, 42] to foster exploration of diverse states. Expanding on this idea, [33] proposed a secondary GFlowNet, driven by intrinsic rewards, to help the primary GFlowNet better approximate the target distribution. DGFN [31] is another approach that involves an auxiliary GFlowNet that is responsible for sampling trajectories, similar to DDQN [53]. In an effort to enhance exploration, [44] adapted Thompson sampling for GFlowNets. Another approach, suggested by [27], involves refining

training trajectories using a local search algorithm before presenting them to the GFlowNet for learning.

4 Methodology

In this section, we describe our methodology for improving the training efficiency and exploration capabilities of GFlowNets. We begin by illustrating a minimal environment that highlights the limitations of on-policy GFlowNet training in discovering high-reward modes. Building on this insight, we introduce a novel training framework that leverages an auxiliary GFlowNet guided by the main GFlowNet’s loss to promote exploration in underrepresented regions of the state space. Finally, we discuss the practical benefits of this loss-guided auxiliary mechanism, particularly in settings where neural network generalization and efficient credit assignment are critical.

4.1 Motivation

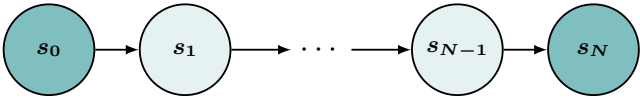


Figure 1: Directed chain of $N + 1$ states. Extremal nodes s_0 and s_N have high reward, while all intermediate states have low reward.

To understand why GFlowNets can fail to learn the desired distribution, we consider a simple illustrative environment, depicted in Figure 1. The state space is defined as $\mathcal{S} = s_0, s_1, \dots, s_N \cup s_f$, and the action space is $\mathcal{A} = \text{advance}, \text{exit}$. For every $i \leq N$, the action `exit` leads from s_i to the terminal state s_f , and for every $i < N$, the action `advance` leads from s_i to s_{i+1} . The reward function assigns high values to the extremal states, with $R(s_0) = R(s_N) \gg R(s_i)$ for all $i \in 1, \dots, N - 1$. We use a tabular GFlowNet where each state s is mapped to a parameter θ_s such that $P_F(\text{exit}|s) = \sigma(\theta_s)$ (where σ is the sigmoid function) and a parameter Z represents the total reward learned.

Despite its simplicity—the environment has a linear, non-branching DAG structure, a single non-terminal action, and a binary reward pattern—training a GFlowNet in an on-policy manner on this environment fails to converge within a reasonable number of iterations. Intuitively, for the GFlowNet to approximate the correct distribution, it must discover and propagate the high reward associated with s_N . However, assuming the initial policy is a uniform action policy where each action is chosen with probability 0.5, the probability of reaching s_N is 0.5^N . This probability diminishes exponentially with N , and as training progresses, the policy increasingly

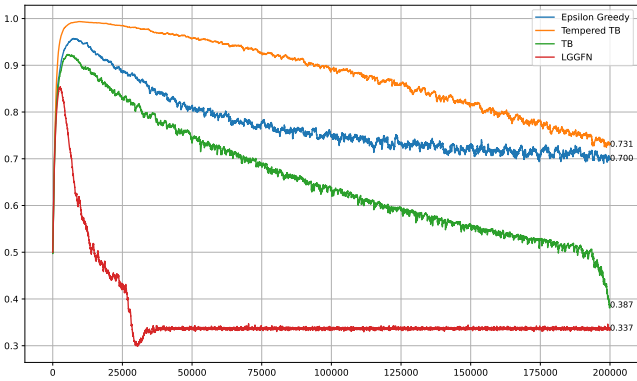


Figure 2: Plot of the evolution of $P_F(\text{exit} | s_0)$ for different algorithms. The chain has 100 states and uses the reward setup $R(s_0) = R(s_N) = 101$ and $R(s_i) = 1$. At convergence, $P_F(\text{exit} | s_0) = \frac{101}{300} \approx 0.337$.

Algorithm 1 Training with Auxiliary GFlowNet

- 1: **Initialize:** Main GFlowNet F_{main} , Auxiliary GFlowNet F_{aux} , reward function R , auxiliary weight λ
- 2: **for** each training iteration **do**
- 3: Sample trajectories $\tau_{\text{aux}} \sim F_{\text{aux}}$
- 4: Sample trajectories $\tau_{\text{main}} \sim F_{\text{main}}$
- 5: Compute loss $\mathcal{L}(\tau_{\text{aux}}, F_{\text{main}}, R)$
- 6: Compute auxiliary reward: $R_{\text{aux}} = R + \lambda \mathcal{L}(\tau_{\text{aux}}, F_{\text{main}}, R)$
- 7: Update F_{aux} using $\mathcal{L}(\tau_{\text{aux}}, F_{\text{aux}}, R_{\text{aux}})$
- 8: Concatenate trajectories: $\tau = \tau_{\text{main}} \cup \tau_{\text{aux}}$
- 9: Update F_{main} using $\mathcal{L}(\tau, F_{\text{main}}, R)$
- 10: **end for**

prioritizes the more easily discovered high-reward state s_0 , further reducing the chance of ever reaching s_N . As a result, s_N is typically discovered far later than expected (approximately 190,000 trajectories in the case of a chain of length 100, as indicated by a noticeable inflection point in the green curve in Figure 2), which significantly slows down learning despite the simplicity of the environment.

In more complex settings where rewards vary more widely, a similar phenomenon can occur: trajectories may get trapped in suboptimal regions around locally high-reward states, further impeding exploration and slowing down convergence.

4.2 Algorithm

In the example illustrated in Figure 1, once the model has learned to terminate trajectories at s_0 , such trajectories become dominant, making the discovery of the final state slower. Figure 2 shows that even after 200,000 trajectories, training using an on-policy method (TB) has yet to converge for a 100-sized chain. Moreover, standard exploration techniques such as tempering or ϵ -greedy exploration prove insufficient in overcoming this limitation.

To address this, we propose training the main GFlowNet using trajectories sampled from an auxiliary GFlowNet, which is optimized to sample trajectories according to a modified reward:

$$R_{\text{aux}} = R_{\text{main}} + \lambda \mathcal{L}_{\text{main}},$$

where R_{main} is the original reward used to train the main GFlowNet, and $\mathcal{L}_{\text{main}}$ denotes the loss associated with a state or trajectory under the main GFlowNet. This auxiliary reward prioritizes trajectories that the main GFlowNet has not yet learned (i.e., those with high loss), while reducing focus on already well-learned regions (i.e., low-loss trajectories). Even if we mainly focus on trajectory-based objective, the same idea holds for transition, state or sub-trajectory based objective. As a result, this encourages broader exploration and mitigates mode collapse.

To leverage the auxiliary GFlowNet, we train the main agent using a mixture of on-policy trajectories and trajectories sampled by the auxiliary GFlowNet. This strategy helps the main agent retain knowledge of previously discovered modes while also exposing it to regions where its performance remains weak. To ensure training stability, we include R_{main} in the auxiliary reward to provide a consistent structural signal, thereby counteracting the inherent fluctuations of the loss term. The coefficient λ balances the influence of the loss and the reward, ensuring that the overall scale of R_{aux} remains comparable to that of R_{main} and avoids destabilizing the learning process. The training procedure is outlined in detail in Algorithm 1.

4.3 Benefits of loss-guided auxiliary GFlowNet

Using the loss of the main GFlowNet as a guide for the auxiliary GFlowNet allows to leverage the generalization induced by the use of Neural Networks. During training, neural networks learn to recognize patterns and generalize them to previously unseen states. For instance, as discussed in Section 5.2, the model may infer that when a sequence is incomplete but valid, the optimal next action leading to high-reward states is consistently appending a 0. Due to this generalization, some trajectories or transitions—despite never being explicitly encountered—can still produce a low loss. Leveraging the loss to guide exploration takes advantage of this property.

In contrast, relying solely on novelty-based intrinsic rewards might drive the model toward areas that are technically new but were already implicitly understood through the network’s generalization. Using the loss is also cheaper computationally, since it will be computed anyway to backpropagate on the main agent, whereas intrinsic rewards ask for a separate set of calculations, and can be expensive depending on which novelty-based algorithm is used.

While similar in spirit, the reward formulation proposed in Kim et al. [28] differs in two aspects. First, it is asymmetric, placing greater emphasis on trajectories where the estimated forward reward $ZP_F(\tau)$ is lower than the expected reward $R(x_\tau)P_B(\tau | x_\tau)$. Second, it combines the primary and auxiliary objectives multiplicatively, using the formulation $\log \mathcal{R}_{\text{aux}} = \alpha \log \mathcal{R} + \log \mathcal{L}$. However, our experiments indicate that this added complexity does not lead to improved performance. In fact, our simplified variant outperforms it by a small margin.

5 Experiments

In the experiments section, we compare three GFlowNets training procedures with the trajectory balance objective: on-policy (that we simply refer to as TB), Siblings Augmented GFlowNet [33] (SAGFN), and our loss-guided auxiliary GFlowNet (LGGFN). We first validate the ability of both SAGFN and LGGFN to discover all modes in the grid, then we show that LGGFN outperforms SAGFN in settings where the rewards have a strong structure, as we predicted in 4.3.

5.1 Hypergrid

The Hypergrid environment, introduced in [4], is a standard setup in GFlowNet literature. In this environment, states are represented as integer vectors corresponding to points in a grid, and actions involve incrementing one of the coordinates. The reward function typically assigns higher values to the corners of the grid (for more details, refer to Appendix A.1.1). To showcase that getting stuck in a mode is one of the main reasons GFlowNets fail to explore the state space, we present a thorough experimentation on the Hypergrid environment.

5.1.1 Comparison between LGGFN and adaptive teachers:

As discussed in Section 4.3, Kim et al. [28] propose a related approach. In this section, we present experimental results demonstrating that our simpler method performs on par with their more complex formulation. Therefore, for the remainder of our experiments, we adopt our version of the loss-guided auxiliary GFlowNet.

Table 1: Final smoothed ℓ_1 distance (scaled by $\times 10^{-5}$) on Hypergrid benchmarks. LGGFN outperforms Adaptive Teacher [28] across grid sizes.

Method	Grid Size		
	32×32	64×64	128×128
Adaptive Teacher	7.20 ± 2.00	2.20 ± 0.31	0.92 ± 0.36
LGGFN	5.33 ± 1.89	2.13 ± 0.61	0.83 ± 0.21

Additionally, we observed that the performance and stability of the original method were highly dependent on the selection of hyperparameters. Specifically, deviations from the hyperparameter values specified in the original work frequently led to numerical instability and NaN values, particularly for larger grid sizes (128 x 128). In contrast, our version exhibits a significantly lower sensitivity to hyperparameter variations, as demonstrated in Section 5.1.4.

5.1.2 Different sizes:

As shown by the toy example in Section 4.1, the size of the environment exponentially impacts the ability of the model to escape explored modes. We validate this observation with a much more complete experimentation. In the following experiments, we use a sparse reward that is difficult to explore ($R_0 = 0.0001$, see Appendix A.1.1 more details).

Table 2: Final smoothed ℓ_1 distance (scaled by $\times 10^{-6}$) for various Hypergrid sizes. Lower is better.

	TB	SAGFN	LGGFN
Size	2-Dimensional Grid		
32	1460.00 ± 0.016	63.9 ± 12.4	53.3 ± 18.9
64	366.00 ± 0.010	24.8 ± 5.64	21.3 ± 6.14
80	234.00 ± 0.0039	17.5 ± 4.51	15.7 ± 3.44
96	163.00 ± 0.0070	11.4 ± 3.09	10.6 ± 1.95
128	91.6 ± 0.0008	7.07 ± 1.00	8.30 ± 2.10
144	72.3 ± 0.0009	2.71 ± 0.493	2.57 ± 0.373
	4-Dimensional Grid		
4	113.0 ± 39.9	169.0 ± 47.7	113.0 ± 58.9
8	417.0 ± 38.2	27.1 ± 5.04	21.2 ± 3.19
16	28.6 ± 0.000099	2.15 ± 0.314	2.13 ± 0.309

We observe that on-policy training quickly becomes ineffective as the size of the hypergrid increases, as it struggles to escape the first mode within a reasonable amount of time. In contrast, both SAGFN and LGGFN perform similarly on this task: they consistently discover all the modes and achieve nearly identical L1 losses across all experiments. For these two algorithms, we can distinguish two distinct training phases. The first phase is characterized by a steep decline in the loss curve, indicating active exploration and significant influence from the auxiliary GFlowNet’s loss or intrinsic reward. The second phase begins when the curve starts to plateau, with only slow, incremental improvement—at this point, the loss or intrinsic reward has diminished to the extent that switching to on-policy training would yield comparable results. It is also worth noting that LGGFN shows more consistent training behavior during the first phase across experiments with different random seeds, as evidenced by a smaller

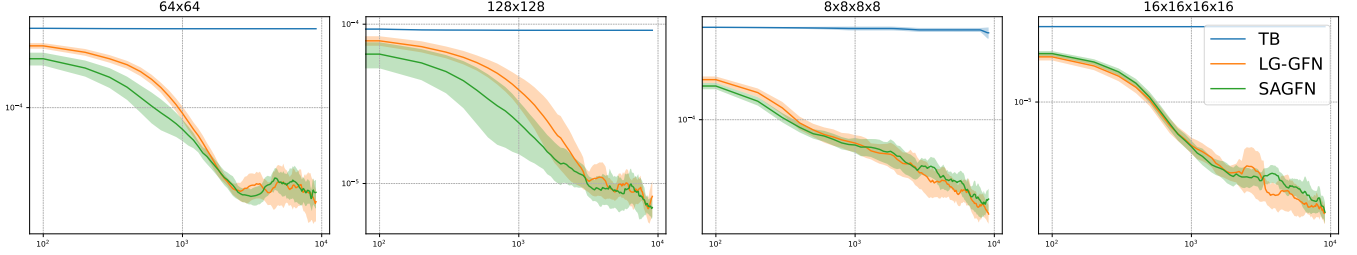


Figure 3: Time evolution of L1-loss during training for different sizes of hypergrid. TB refers to vanilla on-policy training, SAGFN and LGGFN to siblings augmented and loss guided GFlowNets respectively.

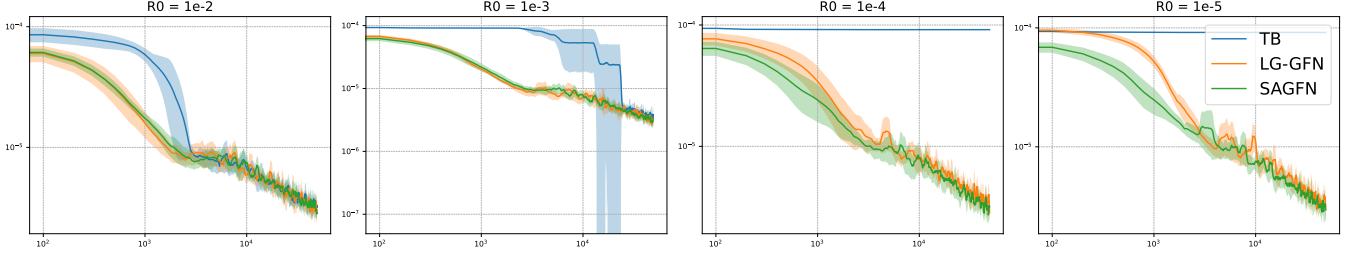


Figure 4: Time evolution of L1-loss during training for different values of R_0 and a fixed size of 128x128.

standard deviation (reflected by the narrower standard deviation band in the plot) compared to SAGFN.

5.1.3 Different sparsity

In the toy example, the main reason the GFlowNet couldn't access the last high reward state is the low reward of the intermediate states, that led to a low move-on probability in the initial state. To validate this hypothesis, we evaluate a range of reward configurations with varying levels of sparsity by systematically modifying the value of R_0 (Figure 4).

We observe that, even in relatively easy settings, on-policy training results in delayed convergence. Furthermore, once all modes have been discovered, the behavior of all three algorithms converges, suggesting that the auxiliary agent can be discarded at this stage. This allows continued on-policy training without performance degradation, while reducing computational overhead.

5.1.4 Influence of the coefficient λ

The auxiliary reward incorporates a coefficient λ to balance the original reward R and the additional loss term \mathcal{L} . However, experimental results indicate that when \mathcal{L} is initially scaled to be in the same range as R , variations in λ within a reasonable range (i.e., not approaching zero) have negligible effect on performance, as demonstrated in Figure 5.

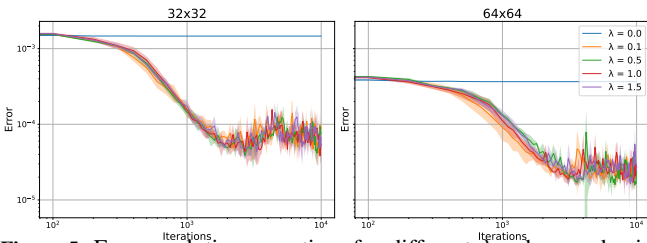


Figure 5: Error evolution over time for different λ values and grid sizes.

5.2 Valid bit sequences

The BITSEQUENCES environment was introduced as a testbed for studying structured sequence generation by Malkin et al. [34], .

Each state in the environment corresponds to a binary sequence, and the agent's actions consist of appending either individual bits or blocks of bits to the current sequence. Episodes start with an empty sequence $s_0 = \epsilon$ and terminate when the sequence reaches a predefined length. In the original formulation, the reward function quantifies how close a given sequence is to the set of modes $R(s) = e^{-d(s, \text{modes})}$. This set of modes is constructed by first arbitrarily selecting a set of words H and then generating different complete sequences by randomly combining these words. Malkin et al. [34] argues that this construction inherently imposes a structural property on the reward function. However, this claim is not entirely accurate, as the candidate sequences that were not ultimately selected as modes still share the same underlying structure but may receive a significantly lower reward. For example, if we work on sequences of size 6 and the set of arbitrary words is $H = \{01, 10\}$ and the set of modes is $\{010101, 101010, 100110\}$. In this setting, the sequence 011001 shares the same "structure" of the modes as it is built from the same process but has a much lower reward e^{-2} (the reward of the modes being 1).

We introduce a new reward structure for this environment (the motivation behind this modification is given in Appendix A.1.2). The set of valid sequences is defined recursively as the smallest set that contains the empty sequence, is closed under concatenation, and is stable under the simultaneous operation of prepending a 0 and appending a 1. Interpreting 0 as an opening parenthesis (and 1 as a closing parenthesis), a valid sequence corresponds to a balanced parentheses sequence. When considering sequences of maximum length $2N$, we define a sequence as *complete* if it attains this maximum length. The objective of the task is to train a GFlowNet to discover the full set of complete valid sequences.

To evaluate the performance of different algorithms in this environment, we sample 16,000 sequences and assess them using two key metrics:

- **Exploration:** We estimate the probability mass assigned to the set of complete valid sequences using Monte Carlo sampling and compare it to the true probability mass.
- **Diversity:** We measure the fraction of distinct complete valid sequences sampled. For sequences of length $2N$, the number of pos-

Table 3: Comparison of on-policy (TB), SAGFN, and LGGFN across different sequence sizes.

Method	16		24		32		40		48	
	Diversity \uparrow	Exploration \downarrow	Diversity \uparrow	Exploration \downarrow	Diversity \uparrow	Exploration \downarrow	Diversity \uparrow	Exploration \downarrow	Diversity \uparrow	Exploration \downarrow
TB	23 \pm 3	0.92 \pm 0.00	15309 \pm 40	0.01 \pm 0.00	23 \pm 3	0.92 \pm 0.00	89 \pm 7	0.99 \pm 0.00	54 \pm 5	0.99 \pm 0.00
SAGFN	473 \pm 640	0.63 \pm 0.41	7387 \pm 95	0.05 \pm 0.01	4392 \pm 3129	0.45 \pm 0.39	102 \pm 13	0.98 \pm 0.01	35 \pm 8	0.99 \pm 0.01
LGGFN	1425 \pm 2	0.01 \pm 0.01	7770 \pm 10	0.01 \pm 0.01	7805 \pm 39	0.02 \pm 0.01	7746 \pm 53	0.02 \pm 0.01	7553 \pm 65	0.05 \pm 0.01

Table 4: Comparison of on-policy (TB), SAGFN, and LGGFN on ROC AUC and SHD metrics across different graph sizes.

Method	Graph Size (Nodes)								
	5	6	7	8	9	10	11	12	13
ROC AUC									
TB	0.72 \pm 0.08	0.57 \pm 0.15	0.58 \pm 0.08	0.60 \pm 0.06	0.53 \pm 0.07	0.53 \pm 0.13	0.56 \pm 0.09	0.52 \pm 0.08	0.56 \pm 0.05
SAGFN	0.66 \pm 0.15	0.68 \pm 0.10	0.44 \pm 0.07	0.51 \pm 0.16	0.56 \pm 0.13	0.59 \pm 0.06	0.49 \pm 0.03	0.52 \pm 0.08	0.55 \pm 0.04
LGGFN	0.57 \pm 0.18	0.68 \pm 0.05	0.62 \pm 0.16	0.52 \pm 0.08	0.57 \pm 0.05	0.62 \pm 0.07	0.63 \pm 0.11	0.59 \pm 0.03	0.57 \pm 0.07
E-SHD									
TB	7.33 \pm 1.08	12.28 \pm 1.06	16.69 \pm 0.12	20.25 \pm 2.62	29.52 \pm 2.11	37.31 \pm 3.97	42.60 \pm 3.38	54.09 \pm 0.41	64.20 \pm 3.05
SAGFN	7.62 \pm 0.23	11.13 \pm 0.85	18.03 \pm 0.49	23.19 \pm 2.20	29.34 \pm 2.60	36.53 \pm 1.12	45.58 \pm 0.76	52.88 \pm 4.78	63.31 \pm 3.77
LGGFN	7.12 \pm 1.38	11.83 \pm 0.37	15.81 \pm 2.47	23.78 \pm 1.36	29.11 \pm 1.17	36.68 \pm 0.63	41.33 \pm 3.50	51.77 \pm 3.50	63.00 \pm 4.50

sible valid bit sequences is given by the Nth catalan number:

$$C_N = \frac{1}{N+1} \binom{2N}{N} = \frac{(2N)!}{(N+1)!N!}. \quad (9)$$

The results are presented in Table 3. Overall, LGGFN significantly outperforms the other algorithms, particularly on longer sequences. Its advantage over SAGFN is likely attributable to its ability to leverage generalization, as hypothesized in Section 4.3.

5.3 Bayesian structure learning

Bayesian networks [43] are probabilistic graphical models that represent a set of variables and their conditional dependencies using a directed acyclic graph (DAG). When this graph is not known *a priori* (e.g., from expert knowledge), it can be inferred from a dataset of observations \mathcal{D} .

Traditional algorithms for this task typically return a single DAG [10], which is suboptimal in practice. One reason for this limitation is that such methods fail to account for the inherent uncertainty arising from Markov equivalence. Two graphs G_1 and G_2 are said to be Markov equivalent if they encode the same set of conditional independencies (Figure 6):

$$G_1 \sim G_2 \Leftrightarrow CI(G_1) = CI(G_2)$$

where $CI(G) = \{(X, Y, Z) \mid X \perp\!\!\!\perp Y \mid Z \text{ in } G\}$

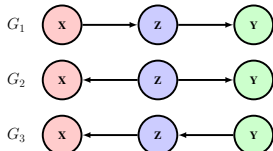


Figure 6: Three Markov equivalent DAGs.

Graphs within the same equivalence class are therefore indistinguishable solely on observational data. Another important consideration is that, when the dataset \mathcal{D} is limited, it may not provide sufficient evidence to clearly favor a particular equivalence class. In such

cases, predicting a single graph (or a single equivalence class) may lead to poor calibration. Hence, it is more appropriate to estimate a posterior distribution over DAGs, $P(G \mid \mathcal{D})$, which better captures the range of plausible graph structures supported by the data.

The use of GFlowNets for Bayesian structure learning was previously explored by Deleu et al. [14], yielding strong empirical results. Building on this work, we evaluate the effectiveness of various algorithms in the context of Bayesian structure learning. To this end, we first generate a random directed acyclic graph (DAG) (by sampling an Erdős–Rényi graph and assigning edge directions such that the source node has a lower index than the target node) and then simulate a dataset consistent with its structure (see Appendix A.1.3 for further details).

In this setting, the states of the environment correspond to DAGs, while the actions consist of adding valid edges—i.e., those that preserve acyclicity. The reward function for a given graph is defined based on the graph itself and its parent graphs in the state space:

$$\log R(G) = \sum_{j=1}^d \text{LocalScore}(X_j \mid \text{Pa}_G(X_j)),$$

where LocalScore denotes the BGe score [19], and $\text{Pa}_G(X_j)$ represents the set of parents of node X_j in graph G .

We evaluate the models using two metrics:

- **Expected Structural Hamming Distance (E-SHD):** the number of missing or extra edges, and the number of reversals required to transform one graph into another.
- **ROC-AUC:** measures how well the predicted edge probabilities distinguish real edges from non-existent edges.

In our experiments, we use synthetic data generated from a known ground-truth structure. We first construct a directed acyclic graph (DAG) by sampling an Erdős–Rényi random undirected graph and orienting each edge from the node with the lower index to the node with the higher index to ensure acyclicity. Data is then generated according to a linear-Gaussian Structural Causal Model (SCM):

$$X_i = \sum_{j \in \text{Pa}(i)} X_j + \varepsilon_i, \quad \varepsilon_i \sim \mathcal{N}(0, \sigma^2),$$

Table 5: Approximate number of Directed Acyclic Graphs (DAGs) for different node counts

# Nodes	5	6	7	8	9	10	11	12	13
# DAGs	2.93×10^4	3.78×10^6	1.14×10^9	7.84×10^{11}	1.21×10^{15}	4.18×10^{18}	3.16×10^{22}	5.22×10^{26}	1.87×10^{31}

where $\text{Pa}(i)$ denotes the set of parents of node i in the DAG, and summation over an empty set is defined to be zero.

Experimental results are presented in Table 4. For graphs with a small number of nodes (5 to 8), all three algorithms exhibit competitive performance, with no single method consistently outperforming the others. However, LGGFN demonstrates a clear advantage as the graph size increases (9 nodes and above). Given that the size of the state space grows rapidly with the number of nodes (see Table 5), this performance gap is likely due to LGGFN’s ability to leverage generalization effectively. By learning to identify and avoid unpromising regions of the search space, LGGFN reduces the need for exhaustive exploration, directly leading to better results.

6 Conclusion

In this work, we introduced Loss-Guided GFlowNets (LGGFN), a simple yet effective auxiliary training strategy for GFlowNets. Through extensive experiments across three distinct domains, we demonstrated that LGGFN consistently improves exploration and sample efficiency over both on-policy trajectory balance (TB) and the previously proposed Siblings Augmented GFlowNet (SAGFN).

The primary limitation of the proposed method lies in the reward function of the auxiliary GFlowNet, \mathcal{R}_{aux} , which depends on the entire trajectory. This contrasts with the standard GFlowNet framework, which is designed to learn a distribution proportional to a reward that depends solely on the terminal state $x \in \mathcal{X}$ (even in cases where the reward is stochastic, the learned distribution is expected to be proportional to the expected reward, $\mathbb{E}[\mathcal{R}(x)]$, again based only on the terminal state).

A promising alternative is to consider a different signal that better indicates whether a state has been effectively learned. One such candidate is the quantity $P_T(x)Z - \mathcal{R}(x)$, which satisfies both criteria: it is a function of the terminal state only, and it directly reflects how close the model is to achieving its goal—learning a distribution proportional to the reward. However, computing the marginal distribution P_T learned by the model is computationally expensive, limiting the practicality of this approach for training purposes. Future work may also explore architectural choices, such as sharing the backbone between the main and auxiliary agents while allowing only the final layer to differ.

References

- [1] P. Auer, N. Cesa-Bianchi, and P. Fischer. Finite-time analysis of the multiarmed bandit problem. *Machine learning*, 47:235–256, 2002.
- [2] Y. Bai, C. Jin, and T. Yu. Near-optimal reinforcement learning with self-play. In H. Larochelle, M. Ranzato, R. Hadsell, M. Balcan, and H. Lin, editors, *Advances in Neural Information Processing Systems*, volume 33, pages 2159–2170. Curran Associates, Inc., 2020.
- [3] M. Bellemare, S. Srinivasan, G. Ostrovski, T. Schaul, D. Saxton, and R. Munos. Unifying count-based exploration and intrinsic motivation. *Advances in neural information processing systems*, 29, 2016.
- [4] E. Bengio, M. Jain, M. Korablyov, D. Precup, and Y. Bengio. Flow network based generative models for non-iterative diverse candidate generation. *Advances in Neural Information Processing Systems*, 34:27381–27394, 2021.
- [5] Y. Bengio, S. Lahlou, T. Deleu, E. J. Hu, M. Tiwari, and E. Bengio. Gflownet foundations. *Journal of Machine Learning Research*, 24(210): 1–55, 2023.
- [6] Y. Bengio, S. Lahlou, T. Deleu, E. J. Hu, M. Tiwari, and E. Bengio. Gflownet foundations. *Journal of Machine Learning Research*, 24(210): 1–55, 2023.
- [7] Y. Burda, H. Edwards, A. Storkey, and O. Klimov. Exploration by random network distillation. In *International Conference on Learning Representations*, 2019.
- [8] O. Chapelle and L. Li. An empirical evaluation of thompson sampling. *Advances in neural information processing systems*, 24, 2011.
- [9] C. Chen, W. Ye, Y. Zuo, C. Zheng, and S. P. Ong. Graph networks as a universal machine learning framework for molecules and crystals. *Chemistry of Materials*, 31(9):3564–3572, 2019. doi: 10.1021/acs.chemmater.9b01294.
- [10] D. M. Chickering. Optimal structure identification with greedy search. *Journal of machine learning research*, 3(Nov):507–554, 2002.
- [11] F. Cipcigan, J. Booth, R. N. Barros Ferreira, C. Ribeiro dos Santos, and M. Steiner. Discovery of novel reticular materials for carbon dioxide capture using gflownets. *Digital Discovery*, 3:449–455, 2024.
- [12] H. M. Cobb. *The History of Stainless Steel*. ASM International, Materials Park, OH, 2010. ISBN 9781615030530.
- [13] S. Curtarolo, G. L. W. Hart, M. B. Nardelli, N. Mingo, S. Sanvito, and O. Levy. The high-throughput highway to computational materials design. *Nature Materials*, 12(3):191–201, 2013. doi: 10.1038/nmat3568.
- [14] T. Deleu, A. Góis, C. Emezue, M. Rankawat, S. Lacoste-Julien, S. Bauer, and Y. Bengio. Bayesian structure learning with generative flow networks. In *Uncertainty in Artificial Intelligence*, pages 518–528. PMLR, 2022.
- [15] A. Ecoffet, J. Huizinga, J. Lehman, K. O. Stanley, and J. Clune. Go-explora: a new approach for hard-exploration problems. *arXiv preprint arXiv:1901.10995*, 2019.
- [16] P. M. Ghari, A. M. Tseng, G. Eraslan, R. Lopez, T. Biancalani, G. Scalia, and E. Hajiramezanali. GFlowNet assisted biological sequence editing. In *The Thirty-eighth Annual Conference on Neural Information Processing Systems*, 2024.
- [17] F. Häse, L. M. Roch, C. Kreisbeck, and A. Aspuru-Guzik. Phoenix: A bayesian optimizer for chemistry. *ACS Central Science*, 4(9):1134–1145, 2018. doi: 10.1021/acscentsci.8b00307.
- [18] F. Häse, M. Aldeghi, R. J. Hickman, L. M. Roch, and A. Aspuru-Guzik. Gryffin: An algorithm for bayesian optimization of categorical variables informed by expert knowledge. *Applied Physics Reviews*, 8(3):031406, 2021. doi: 10.1063/5.0048164.
- [19] D. Heckerman, D. Geiger, and D. M. Chickering. Learning bayesian networks: The combination of knowledge and statistical data. *Machine learning*, 20:197–243, 1995.
- [20] J. Heinrich and D. Silver. Deep reinforcement learning from self-play in imperfect-information games. *arXiv preprint arXiv:1603.01121*, 2016.
- [21] M. Ho, V. Zhu, X. Chen, M. Jain, N. Malkin, and E. Zhang. Proof flow: Preliminary study on generative flow network language model tuning for formal reasoning. In *The First Workshop on System-2 Reasoning at Scale, NeurIPS’24*, 2024.
- [22] E. J. Hu, M. Jain, E. Elmoznino, Y. Kaddar, G. Lajoie, Y. Bengio, and N. Malkin. Amortizing intractable inference in large language models. In *The Twelfth International Conference on Learning Representations*, 2024.
- [23] J. P. Hughes, S. Rees, S. B. Kalindjian, and K. L. Philpott. Principles of early drug discovery. *British Journal of Pharmacology*, 162(6):1239–1249, 2011. doi: 10.1111/j.1476-5381.2010.01127.x.
- [24] M. Jain, E. Bengio, A. Hernandez-Garcia, J. Rector-Brooks, B. F. Dos-sou, C. A. Ekbote, J. Fu, T. Zhang, M. Kilgour, D. Zhang, et al. Biological sequence design with gflownets. In *International Conference on Machine Learning*, pages 9786–9801. PMLR, 2022.
- [25] M. Jiralerspong, B. Sun, D. Vucetic, T. Zhang, Y. Bengio, G. Gidel, and N. Malkin. Expected flow networks in stochastic environments and two-player zero-sum games. In *The Twelfth International Conference on Learning Representations*, 2024.
- [26] J. Jumper, R. Evans, A. Pritzel, T. Green, M. Figurnov, O. Ronneberger, K. Tunyasuvunakool, R. Bates, A. Židek, A. Potapenko, A. Bridgland, C. Meyer, S. A. A. Kohl, A. J. Ballard, A. Cowie, B. Romera-Paredes, S. Nikolov, R. Jain, J. Adler, T. Back, S. Petersen, D. Reiman, E. Clancy, M. Zielinski, M. Steinegger, M. Pacholska, T. Berghammer, S. Bodenstein, D. Silver, O. Vinyals, A. W. Senior, K. Kavukcuoglu, P. Kohli, and D. Hassabis. Highly accurate protein structure predic-

- tion with alphafold. *Nature*, 596(7873):583–589, 2021. doi: 10.1038/s41586-021-03819-2.
- [27] M. Kim, T. Yun, E. Bengio, D. Zhang, Y. Bengio, S. Ahn, and J. Park. Local search gflownets. *arXiv preprint arXiv:2310.02710*, 2023.
- [28] M. Kim, S. Choi, T. Yun, E. Bengio, L. Feng, J. Rector-Brooks, S. Ahn, J. Park, N. Malkin, and Y. Bengio. Adaptive teachers for amortized samplers. In *The Thirteenth International Conference on Learning Representations*, 2025.
- [29] D. L. Klayman. Qinghaosu (artemisinin): an antimalarial drug from china. *Science*, 228(4703):1049–1055, 1985. doi: 10.1126/science.3887571.
- [30] S. Lahlou, T. Deleu, P. Lemos, D. Zhang, A. Volokhova, A. Hernández-García, L. N. Ezzine, Y. Bengio, and N. Malkin. A theory of continuous generative flow networks. In *International Conference on Machine Learning*, pages 18269–18300. PMLR, 2023.
- [31] E. Lau, N. Vemgal, D. Precup, and E. Bengio. Dgfn: Double generative flow networks. *arXiv preprint arXiv:2310.19685*, 2023.
- [32] K. Madan, J. Rector-Brooks, M. Korablyov, E. Bengio, M. Jain, A. C. Nica, T. Bosc, Y. Bengio, and N. Malkin. Learning gflownets from partial episodes for improved convergence and stability. In *International Conference on Machine Learning*, pages 23467–23483. PMLR, 2023.
- [33] K. Madan, A. Lamb, E. Bengio, G. Berseth, and Y. Bengio. Towards improving exploration through sibling augmented gflownets. In *The Thirteenth International Conference on Learning Representations*, 2025.
- [34] N. Malkin, M. Jain, E. Bengio, C. Sun, and Y. Bengio. Trajectory balance: Improved credit assignment in gflownets. *Advances in Neural Information Processing Systems*, 35:5955–5967, 2022.
- [35] N. Malkin, S. Lahlou, T. Deleu, X. Ji, E. J. Hu, K. E. Everett, D. Zhang, and Y. Bengio. GFlownets and variational inference. In *The Eleventh International Conference on Learning Representations*, 2023.
- [36] D. C. Manta, E. J. Hu, and Y. Bengio. GFlownets for causal discovery: an overview. In *ICML 2023 Workshop: Sampling and Optimization in Discrete Space*, 2023.
- [37] T. M. Nguyen, S. A. Tawfik, T. Tran, S. Gupta, S. Rana, and S. Venkatesh. Hierarchical gflownet for crystal structure generation. In *AI for Accelerated Materials Design-NeurIPS 2023 Workshop*, 2023.
- [38] L. Pan, N. Malkin, D. Zhang, and Y. Bengio. Better training of gflownets with local credit and incomplete trajectories. In *International Conference on Machine Learning*, pages 26878–26890. PMLR, 2023.
- [39] L. Pan, D. Zhang, A. C. Courville, L. Huang, and Y. Bengio. Generative augmented flow networks. In *ICLR*, 2023.
- [40] L. Pan, D. Zhang, M. Jain, L. Huang, and Y. Bengio. Stochastic generative flow networks. In *The 39th Conference on Uncertainty in Artificial Intelligence*, 2023.
- [41] M. Pandey, G. Subbaraj, and E. Bengio. GFlownet pretraining with inexpensive rewards. In *NeurIPS 2024 Workshop on AI for New Drug Modalities*, 2024.
- [42] D. Pathak, P. Agrawal, A. A. Efros, and T. Darrell. Curiosity-driven exploration by self-supervised prediction. In *International conference on machine learning*, pages 2778–2787. PMLR, 2017.
- [43] J. Pearl. *Probabilistic reasoning in intelligent systems: networks of plausible inference*. Elsevier, 2014.
- [44] J. Rector-Brooks, K. Madan, M. Jain, M. Korablyov, C.-H. Liu, S. Chandar, N. Malkin, and Y. Bengio. Thompson sampling for improved exploration in gflownets. *arXiv preprint arXiv:2306.17693*, 2023.
- [45] K. T. Schütt, H. E. Sauceda, P.-J. Kindermans, A. Tkatchenko, and K.-R. Müller. Schnet—a deep learning architecture for molecules and materials. *The Journal of Chemical Physics*, 148(24):241722, 2018. doi: 10.1063/1.5019779.
- [46] M. Sendera, M. Kim, S. Mittal, P. Lemos, L. Scimeca, J. Rector-Brooks, A. Adam, Y. Bengio, and N. Malkin. Improved off-policy training of diffusion samplers. In *The Thirty-eighth Annual Conference on Neural Information Processing Systems*, 2024.
- [47] T. Shen, S. Seo, G. Lee, M. Pandey, J. R. Smith, A. Cherkasov, W. Y. Kim, and M. Ester. TacoGFN: Target-conditioned GFlownet for structure-based drug design. *Transactions on Machine Learning Research*, 2024. ISSN 2835-8856.
- [48] T. Silva, R. B. Alves, E. de Souza da Silva, A. H. Souza, V. Garg, S. Kaski, and D. Mesquita. When do GFlownets learn the right distribution? In *The Thirteenth International Conference on Learning Representations*, 2025.
- [49] S. Sukhbaatar, Z. Lin, I. Kostrikov, G. Synnaeve, A. Szlam, and R. Fergus. Intrinsic motivation and automatic curricula via asymmetric self-play. In *International Conference on Learning Representations*, 2018.
- [50] R. S. Sutton, A. G. Barto, et al. *Reinforcement learning: An introduction*, volume 1. MIT press Cambridge, 1998.
- [51] R. Takase, M. Tsunokake, Y. Tsuchiya, and S. Inuzuka. Gflownet fine-tuning for diverse correct solutions in mathematical reasoning tasks. *arXiv preprint arXiv:2410.20147*, 2024.
- [52] W. R. Thompson. On the likelihood that one unknown probability exceeds another in view of the evidence of two samples. *Biometrika*, 25(3-4):285–294, 1933.
- [53] H. Van Hasselt, A. Guez, and D. Silver. Deep reinforcement learning with double q-learning. In *Proceedings of the AAAI conference on artificial intelligence*, volume 30, 2016.
- [54] M. C. Wani, H. L. Taylor, M. E. Wall, P. Coggon, and A. T. McPhail. Plant antitumor agents. vi. isolation and structure of taxol, a novel antileukemic and antitumor agent from **taxus brevifolia**. *Journal of the American Chemical Society*, 93(9):2325–2327, 1971. doi: 10.1021/ja00738a045.
- [55] T. Wolf, L. Debut, V. Sanh, J. Chaumond, C. Delangue, A. Moi, P. Cistac, T. Rault, R. Louf, M. Funtowicz, et al. Huggingface’s transformers: State-of-the-art natural language processing. *arXiv preprint arXiv:1910.03771*, 2019.
- [56] D. Zhang, H. Dai, N. Malkin, A. Courville, Y. Bengio, and L. Pan. Let the flows tell: Solving graph combinatorial problems with GFlownets. In *Thirty-seventh Conference on Neural Information Processing Systems*, 2023.
- [57] D. Zhang, Y. Zhang, J. Gu, R. Zhang, J. M. Susskind, N. Jaitly, and S. Zhai. Improving gflownets for text-to-image diffusion alignment. *CoRR*, abs/2406.00633, 2024.
- [58] D. W. Zhang, C. Rainone, M. Peschl, and R. Bondesan. Robust scheduling with GFlownets. In *The Eleventh International Conference on Learning Representations*, 2023.
- [59] T. Zhang, H. Xu, X. Wang, Y. Wu, K. Keutzer, J. E. Gonzalez, and Y. Tian. Noveld: A simple yet effective exploration criterion. *Advances in Neural Information Processing Systems*, 34:25217–25230, 2021.

A Appendix / Supplemental Material

A.1 Experiments

All experiments are run on 3 different seeds and were done using `torchgfn`. For all learnable parameters, the learning rate is set to 0.001, except for the learnable scalar $\log Z$ used in trajectory balance objective, whose learning rate is set to 0.1. After many experiments, this choice seems to work best in general, allowing SAGFN to achieve better results than the ones presented in the original paper [33]. For each GFlowNet, we use the same backbone neural network to learn the forward and backward policy, only changing the final layer to differentiate between them. The auxiliary GFlowNet uses a different backbone network than the main GFlowNet.

A.1.1 Hypergrid

The Hypergrid environment is traditionally trained with the following reward function:

$$R(x) = R_0 + R_1 \prod_i \mathbb{I} \left(0.25 < \left| \frac{x_i}{H} - 0.5 \right| \right) + R_2 \prod_i \mathbb{I} \left(0.3 < \left| \frac{x_i}{H} - 0.5 \right| < 0.4 \right)$$

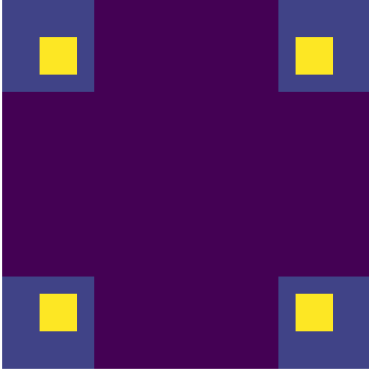


Figure 7: Legend: A 2D Hypergrid environment. States correspond to points $(x_i)_{1 \leq i \leq n}$ on the grid, and actions represent forward transitions in one direction.

We evaluate the task using grid sizes $H \in \{32, 64, 80, 96, 128, 144\}$, across both 2D and 4D configurations, and vary the reward sparsity using $R_0 \in \{0.01, 0.001, 0.0001, 0.00001\}$. The agent is parameterized by a multi-layer perceptron (MLP) consisting of two hidden layers with 256 units each and ReLU activations. After extensive tuning of the regularization hyperparameter λ , we observed that performance remains consistent as long as $\lambda \neq 0$; all results reported in the paper use $\lambda = 1$.

For SAGFN, we use the hyperparameters from original work [33]:

$$\beta_e^{\text{main}} = 1, \quad \beta_e^{\text{aux}} = 0.25, \quad \beta^{\text{aux}} = 1, \quad \beta^{\text{main}} = 1, \quad \beta_i = 1$$

To compare LGGFN against the Adaptive Teacher from [28]:

$$\begin{aligned} \log R_{\text{aux}}(x) &= \log R_{\text{aux}}^{\text{weighted}}(x; \theta) + \alpha \log R(x) \\ \log R_{\text{aux}}^{\text{weighted}}(x; \theta) &= \log (\epsilon + (1 + C \cdot \mathbb{I}[\delta(\tau; \theta) > 0]) \cdot \delta(\tau; \theta)^2) \\ \delta(\tau; \theta) &= \log R(x) + \log P_B(\tau | x) \\ &\quad - (\log Z_\theta + \log P_F(\tau; \theta)) \end{aligned}$$

We use the same hyperparameters as in [28], where $C = 19$ and $\alpha = 0.5$.

A.1.2 Valid sequences

Table 6: Catalan numbers for selected values of N .

N	Catalan Number
8	1430
12	2674440
16	35357670
20	6564120420
24	1289904147324

This task involves generating a binary sequence by autoregressively appending individual bits. Compared to the original BITSEQUENCES environment, several key modifications make this version more challenging:

- **Reward Function:** In contrast to the original setting, which featured unstructured and near-random rewards, the modified environment introduces a structured and sparse reward function. Substantial rewards are allocated exclusively to sequences that are both complete and balanced, while the vast majority of other sequences yield negligible reward. Exploration can be made even more challenging by assigning to small sequences (e.g., those shorter than 4 or 8 bits) deceptively low but nonzero rewards—higher than those of arbitrary incomplete sequences but significantly lower than optimal ones. This design introduces local optima (without affecting much the marginal distribution of the problem) that can mislead inadequately exploratory training strategies, potentially trapping the policy and mimicking the behavior illustrated in Figure 2.
- **Terminating States:** In the original environment, only fully constructed sequences are terminal. Here, the agent may choose an exit action at any sequence length. This change increases task complexity, as the agent must learn to discern whether a partial sequence is promising enough to continue or whether to exit, despite most high-reward sequences occurring only at full length.
- **Word Size:** In the original experiments, sequences had fixed length, and each step appended a binary word of size k , varying across experiments. In our version, sequences terminate upon taking the exit action, and the agent adds one bit at a time. This increases the relative importance of the exit action, which now has a probability of $1/3$ (compared to $1/(2^k + 1)$ when adding k -bit words), making the decision to stop a more frequent and significant consideration.

For this task, we use `GPT2Model` from Hugging Face’s transformers library [55] with 3 hidden layers, 8 attention heads, and embeddings of dimension 64. For LGGFN, λ was set to 1 and for SAGFN, $\{\beta_e^{\text{main}} = 1, \beta_e^{\text{aux}} = 1, \beta^{\text{aux}} = 1, \beta^{\text{main}} = 1, \beta_i = 1\}$.

A.1.3 Bayesian Structure Learning

For this task, we use a directional graph-based neural architecture to compute action logits for graph generation. The model supports decisions for both edge creation between nodes and an optional stop action that signals the end of generation. The network begins by embedding node identifiers into a continuous feature space. These embeddings are processed through multiple layers of direction-aware graph convolutions that distinguish between incoming and outgoing edges. Each layer includes residual connections to preserve information across depths and applies layer normalization to stabilize training. The output of each convolutional layer consists of separate representations for incoming and outgoing directional features. These are

refined independently using small feedforward networks and then recombined into a unified node representation. To produce edge-level action scores, the model computes dot products between the feature vectors of source and target nodes. In addition, a pooled summary of all node embeddings can be used to compute a score for the optional stop action. The final output consists of unnormalized logits representing the desirability of all possible edge additions and, if applicable, the decision to terminate the graph construction process.

Unlike the previous two tasks, this task exhibits significantly higher loss values, often exceeding the magnitude of the actual rewards. Moreover, the loss values vary with the number of nodes in the input graph. To account for this, the hyperparameter λ was selected individually for each graph size by empirically observing the loss range over a series of iterations and then choosing a value of λ that brings the loss scale closer to that of the reward. For the SAGFN model, we adopt the following configuration of weighting coefficients $\{\beta_e^{\text{main}} = 1, \beta_e^{\text{aux}} = 1, \beta_{\text{aux}} = 1, \beta_{\text{main}} = 1, \beta_i = 1\}$. This setup ensures that the intrinsic reward remains within the same range as the extrinsic reward, facilitating more stable training.

A.2 Visualization of HyperGrid learned distributions

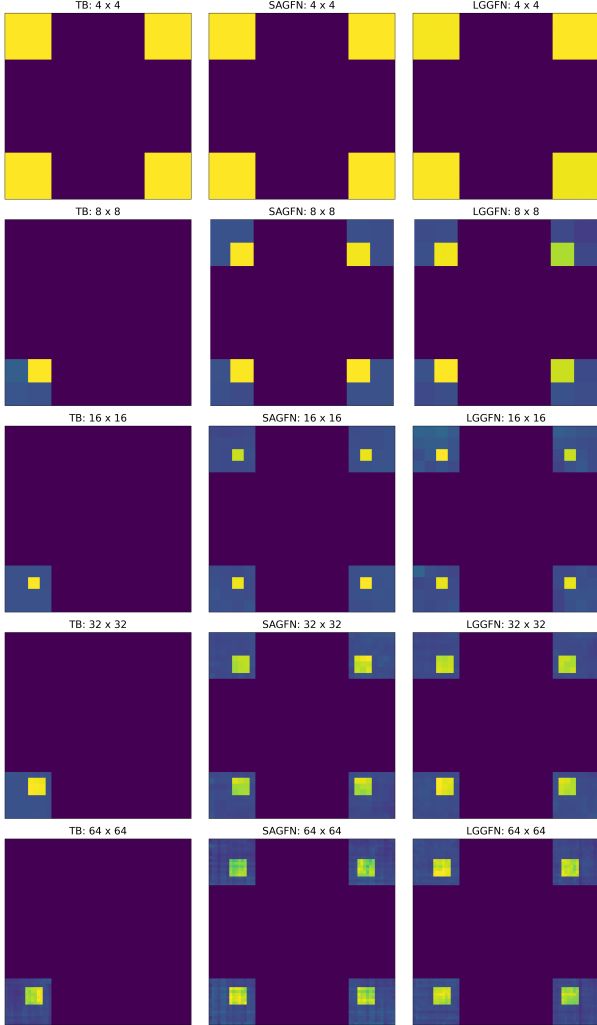


Figure 8: Learnt distributions on environment with size from 4 to 64.

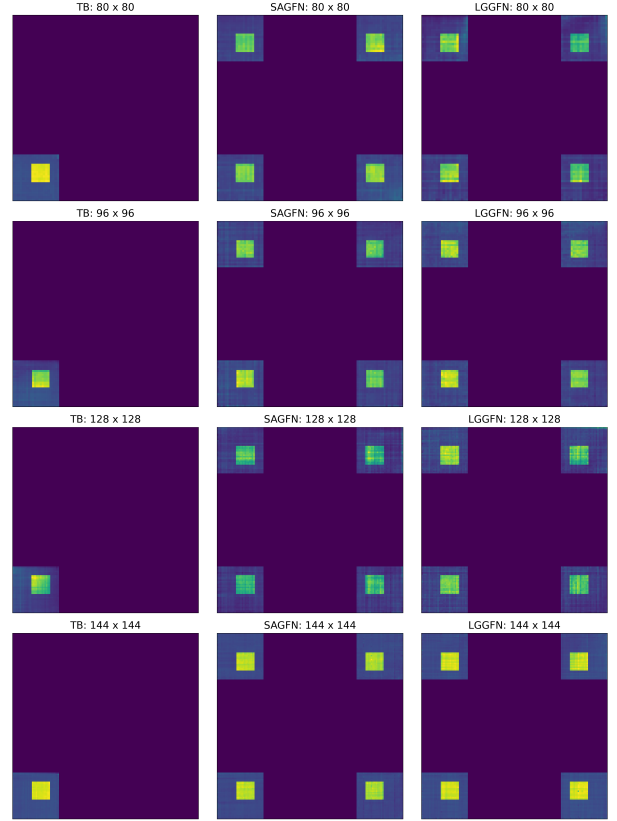


Figure 9: Learned distributions on environment with size from 80 to 144.